JOURNAL OF MATERIALS SCIENCE 24 (1989) 2391–2400

Short-rod elastic–plastic fracture toughness test using miniature specimens

C. T. WANG, R. M. PILLIAR*
Centre for Biomaterials, University of Toronto, 124 Edward Street, Toronto, Ontario M5G 1G6, Canada

The standard ASTM-E399 plane-strain fracture toughness (K_{IC}) test requires (1) the test specimen dimensions to be greater than a minimum size and, (2) fatigue precracking of the specimen. These criteria render many materials impractical to test. The short-rod elastic–plastic plane-strain fracture toughness test proposed by Barker offers a method of testing not requiring fatigue precracking and furthermore, it appears that test specimens smaller than that stipulated by ASTM can be used to obtain valid K_{IC} values. In this study, the use of a modified miniature short-rod fracture toughness test specimen was investigated. Our miniature short-rod specimen is approximately 7 mm long and 4 mm diameter. These mini specimens are well suited for the purpose of testing biomaterials. The value of the minimum stress intensity factor coefficient (Y_m^*) for the mini short-rod specimens was determined experimentally using specimens machined from extruded acrylic rod stock. An elastic–plastic fracture toughness analysis using the mini specimens gave values of K_{IC} for extruded acrylic (nominally PMMA) equal to $0.67 \pm 0.06\,MPa\,m^{1/2}$. The problem of testing non-flat crack growth resistance curve materials (such as PMMA) using the short-rod fracture toughness test method is discussed. A modification to the test procedure involving the use of a Y^* value corresponding to a short crack length is suggested as a method of overcoming this difficulty.

Nomenclature

a	crack length
a_0	initial crack length
a_1	length of the chevron notch on the mini short-rod specimen
a_m	critical crack length − crack length at Y_m^*
C	specimen compliance
C'	dimensionless specimen compliance = CED
D	mini short-rod specimen diameter
E	Young's modulus
K_I	stress intensity factor
K_{IC}	plane-strain fracture toughness
K_{max}	fracture toughness calculated using P_{max}
P	load applied to the test specimen during a short-rod fracture toughness test
P_c	load applied to the test specimen at Y_m^*
P_{max}	maximum load applied to the specimen during a short-rod fracture toughness test
p	plasticity factor
W	mini short-rod specimen width
Y^*	stress intensity factor coefficient
Y_m^*	minimum of the stress intensity factor coefficient
α	dimensionless crack length = a/W
α_0	dimensionless initial crack length = a_0/W
α_1	dimensionless chevron notch length = a_1/W
α_m	dimensionless critical crack length = a_m/W

1. Introduction

It is well recognized that many engineering materials fail in service by fracturing due to the growth of inherent internal flaws. Traditional mechanical tests such as ultimate tensile and compressive strength and unnotched fatigue tests cannot accurately predict the fracture resistance of a material. A more appropriate criterion for characterizing a material's resistance to fracture is fracture toughness, determined by standard tests such as that described by ASTM-E399.

The standard ASTM-E399 plane-strain fracture toughness test requires the test specimen width to be greater than 2.5 $(K_{IC}/\sigma_{ys})^2$, where K_{IC} is the plane-strain fracture toughness and σ_{ys} is the yield strength of the material. Adherence to this condition ensures plane-strain conditions along a major portion of the crack front during testing. This minimum size criterion, however, makes the testing of many high toughness or low yield strength materials impractical. The ASTM test procedure also requires fatigue precracking of the specimen in order to achieve a sharp and reproducible crack tip geometry for testing. This can create difficulties in the testing of many polymeric materials. The short-rod fracture toughness test proposed by Barker [1] offers an alternative fracture toughness test method that can use much smaller test specimens that do not require fatigue precracking. It therefore appears to overcome the difficulties

*Author to whom all correspondence should be addressed.

0022–2461/89 $03.00 + .12

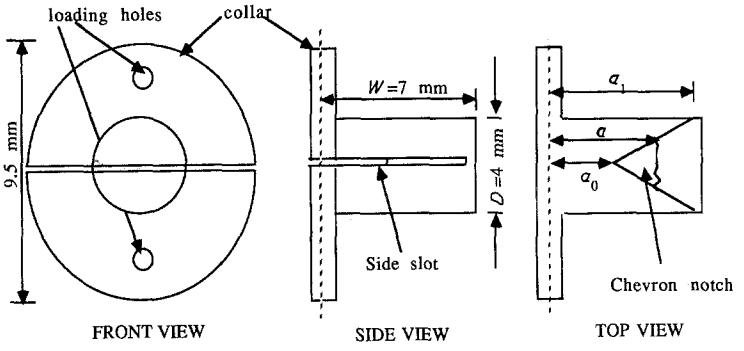

Figure 1 The geometry and the dimensions of the mini short-rod specimens.

associated with the standard test method. The short-rod specimen geometry includes a thin side slot forming a chevron-shaped test region. These thin side slots maintain the test material in a plane-strain state even when using a specimen much smaller in size than that specified by ASTM-E399. The chevron-shaped area of material being tested results in the initiation of a crack at the tip of the chevron that quickly achieves a quasi-static or steady state growth so that fatigue precracking of the test specimen is not necessary. The low load required for crack initiation aids in the testing of brittle materials by reducing the chance of initial catastrophic failure of the specimens. Barker has also proposed an elastic-plastic analysis for short-rod specimens that exhibit significant but limited plastic deformation during testing [2].

Barker's short-rod fracture toughness test method and specimen geometry have been adopted for our study. However, because of our interest in biomaterials and special concerns related to their use and testing, the size of specimen utilized in our tests is smaller than that originally proposed by Barker [1–3]. The nominal dimensions of our miniature short-rod specimens are shown in Fig. 1. The diminutive size of the mini specimens (4 mm diameter) approaches the cross-sectional dimensions of some biomaterials as used clinically. Bone cements and dental composites, for example, are used to fill narrow spaces that can be 4 mm in cross-section. The use of small test specimens also allows *in vivo* ageing of materials by implantation into small inexpensive laboratory animals prior to testing [4].

The use of the miniature short-rod specimen need not be limited to the testing of biomaterials. For example, determination of through-the-thickness variations in toughness in metallic plate or sheet also requires small specimens [5].

A major concern in using smaller than standard specimens for determining plane-strain fracture toughness (K_{IC}) is the effect of the small specimen size on crack zone stress state; i.e. will plane-strain conditions be maintained? In this study, we investigated the use of miniature short-rod test specimens using the elastic–plastic analysis method proposed by Barker [2]. The small size and fragility of the miniature specimens created a special problem for monitoring crack opening displacement. We have resolved this problem by using a non-contacting displacement measuring method, namely laser telemetry, for measuring slot opening during testing. This report describes the elastic–plastic fracture toughness test method developed, and a subsequent paper reports on the application of this method for testing bone cements [6].

1.1. Short-rod fracture toughness testing

For a material having a flat crack growth resistance curve (*R*-curve) deforming in a linear–elastic manner during a short-rod fracture toughness test, the plane-strain fracture toughness can be calculated using the relation [7]

$$K_{IC} = \frac{P_C}{DW^{1/2}} Y_m^* \quad (1)$$

where P_c is the peak load applied to the specimen during an increasing load test, D is the specimen diameter, W is the specimen width and Y_m^* is the minimum of the dimensionless stress intensity factor coefficient that describes the variation of specimen compliance with crack growth (see Equation 3) [7]. An equation of this form was derived by Barker by balancing the energy required to advance the steady-state crack within the chevron-shaped test section and the irrecoverable work done to advance the crack [1]. The simplicity of this method lies in the fact that the only parameter requiring determination during testing is P_c. It has been shown that the factor Y_m^* is independent of the test material as long as it deforms linear-elastically [1, 7]. The value of Y_m^* has been determined both experimentally and analytically for short-rod specimens with similar geometry and size to the specimens proposed by Barker [1–3, 8–13]. Y_m^* has not been determined previously for the mini short-rod specimens that we have used for testing biomaterials [4, 14, 15].

For materials deforming in an elastic–plastic manner, K_{IC} can be determined using the relation [2]

$$K_{IC} = K_q \left(\frac{1+p}{1-p}\right)^{1/2} \quad (2)$$

where K_q is the critical stress intensity factor determined assuming linear-elastic behaviour, i.e. using Equation 1, and p is a factor to account for plasticity. In calculating K_q, however, P_c is no longer the peak load applied to the specimen during the test as in the linear-elastic case. When a specimen behaves elastic–plastically, the peak load generally would not occur at a crack length corresponding to the minimum of Y^*. When using Equation 2, P_c is the load required to advance the crack through the crack length corresponding to Y_m^*. The plasticity factor, p, is calculated from a load–load-point displacement curve determined during the test. The elastic–plastic (EP) test

method is more complex than the linear-elastic (LE) method in that loading–unloading procedures are required during testing and the load–displacement curves must be recorded.

2. Experimental methods

2.1. Material and specimen preparation

A commercially-available extruded acrylic (nominally PMMA) was chosen for our initial study of the mini short-rod EP fracture toughness test. Fracture toughness testing of PMMA has been reported extensively in the literature. This transparent material is also well suited for the determination of Y_m^* because the crack front is easily visible through the specimen, thereby simplifying crack length measurements.

The configuration of our mini short-rod specimen is shown in Fig. 1. The specimen is nominally 7 mm long and 4 mm diameter. To allow specimen loading, a collar 9.5 mm diameter and 1 mm thick with two loading holes is formed as an integral part of the specimen front face. The slot that is machined along the mid-plane of the specimen is approximately 0.25 mm wide and forms a chevron-shaped zone along about one-half the length of the specimen.

The specimens were machined from the extruded rod stock. The two loading holes were drilled in the collar using a hardened steel drill guide. The mid-plane slot was cut into the specimen preform by using a 0.25 mm thick diamond impregnated wafering blade. The chevron-shaped slot was obtained using two coplanar passes of the blade, rotating the specimen through 60° about an axis normal to its long direction between the two passes. The finished specimens were annealed in a forced draft oven at 70° C for 24 h prior to testing. The annealing procedure was intended to remove any differences between individual specimens caused by sample preparation procedures.

2.2. Testing procedures

2.2.1. Determination of compliance calibration curve for mini short-rod specimens

The dimensionless stress intensity factor coefficient, Y^*, is defined as

$$Y^* = \left[\frac{1}{2}\frac{dC'}{da}\frac{\alpha_1 - \alpha_0}{\alpha - \alpha_0}\right]^{1/2} \quad (3)$$

where C' = EDC is the dimensionless compliance and α, α_1 and α_0 are crack and chevron-notch lengths normalized against specimen length. To obtain values of Y^* and, therefore, Y_m^* (the minimum of Y^* as a function of crack length), one must first determine the dependence of C' on crack length as well as Young's modulus, E. Compliance calibration curves (C' against a) and Young's modulus were determined experimentally using acrylic test specimens as described below.

Compliance measurements of the mini specimens were made for different crack lengths. After measuring the initial compliance of the specimen, the tip of the chevron-shaped test area was nicked with a razor blade to facilitate crack initiation. The resulting crack was advanced by monotonically loading the specimen in an Instron universal testing machine (Instron Corp., Canton, Mass., Model TT-CM) until a sharp drop in load corresponding to a crack jump was observed. The crack was progressed approximately 0.02 mm for successive compliance measurements. The crack lengths, as well as the necessary dimensions of each specimen, were measured using a Mitutoyo toolmakers microscope (Mitutoyo Corp., Tokyo, Japan, Model TM-201) under oblique and normal reflected light. The digital micrometer readout attached to the microscope is precise to 0.001 mm. Initially the crack fronts were relatively straight and, therefore, few measurements were taken along the crack front to obtain the average crack length. As the crack propagated into the specimen, however, "thumbnailing", or retardation of the edges of the crack front, was observed. The number of measurements taken were increased as the curvature of the crack front became apparent. At least ten crack length measurements were taken along a curved crack front at regular intervals and the average value was used in the calculations.

For testing, the specimen was held in the loading fixture by passing two drill rods through the loading holes in the specimen collar (Fig. 2). The position of the load line, therefore, was considered to pass along the mid-thickness point on the collar. During specimen loading slot width at the collar was monitored using a non-contacting laser telemetric system (Zygo Corp., Middlefield, Connecticut, model 121) as illustrated in Fig. 2. The transmitted laser beam measured the width of the slot which was detected by the receiver of the laser telemetric system. To avoid measurement errors due to collar thickness effects, a paper-thin veneer sheet was stuck to the front face of the specimen. This sheet provided a lateral extension of the slot on the front face beyond the acrylic specimen proper. The laser beam was directed through the slot in the veneer sheet where it extended beyond the specimen. Both the Instron load-cell amplifier and the laser telemetric system were interfaced with a microcomputer to allow load–load-line slot opening width data to be collected simultaneously and stored on disc.

Prior to testing, a preconditioning procedure to properly seat the specimen within the loading fixture and to ensure that the crack surfaces were completely separated was performed. Preliminary experiments showed that this procedure increased the consistency of the compliance measurements and the linearity of the load-slot opening width curves. This preconditioning procedure involved loading the specimen to approximately 80% of the load required to propagate the crack and holding at this load for several minutes. The specimen was then unloaded and cycled four times at a cross-head speed of 0.02 cm min^{-1} within the load range intended for testing. Testing started immediately after preconditioning with an initial load of 2.5 N being applied to the specimen. After the specimen had been allowed to equilibriate for approximately 1 min with the cross-head of the testing machine stationary, two hundred readings of the load and slot opening at the front face of the specimen were taken. The average values of load and slot opening width were computed and displayed on the computer

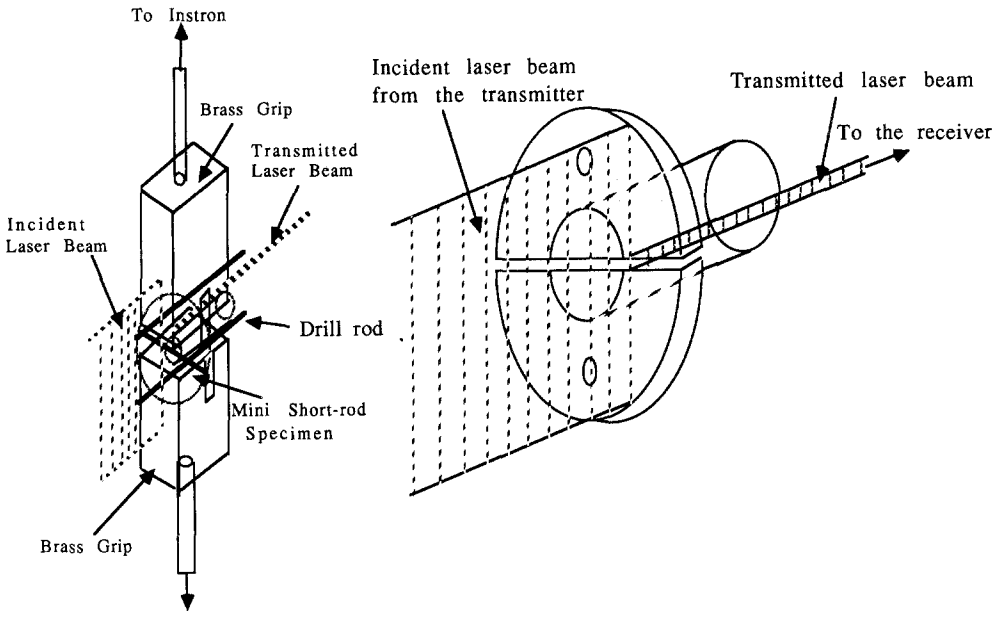

Figure 2 Schematic drawing of the loading and the displacement measuring configuration for compliance measurement and fracture toughness testing of the miniature specimens.

screen. Averages were taken at approximately 1 min intervals until consecutive results within 1% of each other were obtained. The load was then increased by approximately 0.1 N and these procedures repeated. Two loading cycles between 2.5 and 3.5 N were performed for each test run. The specimen was removed from the loading fixture after each test and allowed to relax free of loading for 1 h. A minimum of three tests was performed at each crack length depending upon the scatter of the results.

The load–slot opening width curves (two for each test) were plotted on the computer. The slope (slot opening width/load) of the best-fit straight line through the data points was taken as the compliance of the specimen at that particular crack length. The average compliance from all tests performed at a crack length was used to determine Y^* using Equation 3. Four acrylic mini short-rod specimens were tested successfully.

Young's modulus of the acrylic was determined using the procedures described in ASTM-D638 specification. A type II tensile specimen (Fig. 3) modified for ease of machining was selected. Four test specimens were cut from the same extruded acrylic rod as was used for fabricating the mini short-rod fracture toughness specimens. The tensile specimens were annealed after machining in the same manner as the fracture toughness specimens. The cross-sectional dimension of the specimens along the gauge length was measured using a micrometer prior to the test. Testing was performed on the Instron testing machine and the specimen displacements were measured using an Instron strain gauge extensometer (model GSI-16MA A324-28). Each specimen was loaded and unloaded at least three times at a cross-head speed of 0.02 cm min^{-1} to simulate the experimental compliance calibration conditions. The average slope of all loading curves was used for the calculation of E.

2.2.2. Short-rod elastic-plastic fracture toughness test

The procedure outlined by Barker [2] for short-rod plane-strain fracture toughness testing with correction for plasticity was followed. Annealed acrylic miniature short-rod specimens were tested at room temperature (25 ± 2° C) at a cross-head speed of 0.05 cm min^{-1}. Measurements of load against crack opening displacement, or a displacement directly proportional to it, are required to determine the plasticity factor, p. The measurement of the specimen slot opening width is proportional to the crack opening displacement and was used in our studies. It was measured using the laser telemetric system during fracture toughness testing. A conditioning load–unload cycle (1, Fig. 4) was used to seat the specimen in the grips. The peak load in this conditioning cycle was kept low enough to prevent crack initiation because the slope of the loading portion of the next load–unload cycle was used to determine the initial specimen compliance. Unloading was stopped when a load of 3.0 N was reached. Due to the viscoelastic nature of the test specimen, the load acting on it continued to increase after cross-head movement stopped (2, Fig. 4). The cross-head was restarted (loading/unloading) only when no further

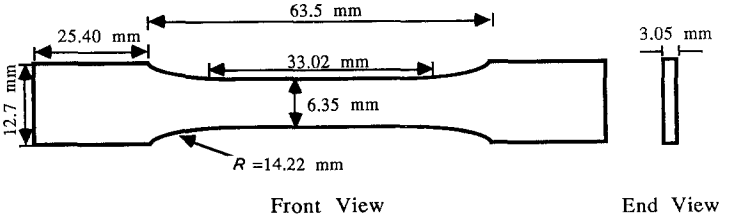

Figure 3 Modified ASTM-D638 type II tensile specimen for the determination of Young's modulus.

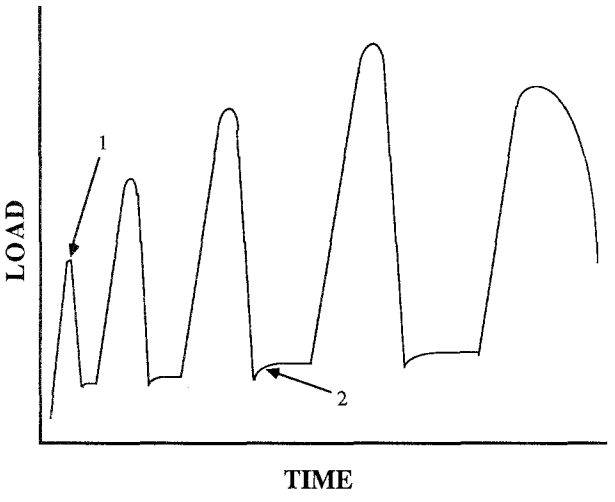

Figure 4 Schematic drawing of a typical load–time curve illustrating short-rod elastic–plastic fracture toughness test procedure.

increase in load was apparent. Three load–unload cycles were performed for each specimen prior to fracturing the specimen. Ideally, these three cycles would bracket the critical crack length (i.e. the crack length at which Y^* is a minimum $= Y_m^*$). Each fracture toughness test took approximately 7 min during which 2000 data points were read and stored by the computer.

Measurements of D and W were made using both halves of the broken specimen after the test using the Mitutoyo toolmakers microscope.

2.3. Analysis procedures

2.3.1. Stress intensity factor coefficient determination

Dimensionless compliance C' plotted against a is shown in Fig. 5. A fourth degree polynomial was fitted to the C' data points. A polynomial was chosen for curve fitting because this function provided good fit to the data and the derivative of this function is easily obtainable for the calculation of Y_m^*. Y^* values were calculated using Equation 3, and a plot of Y^* against

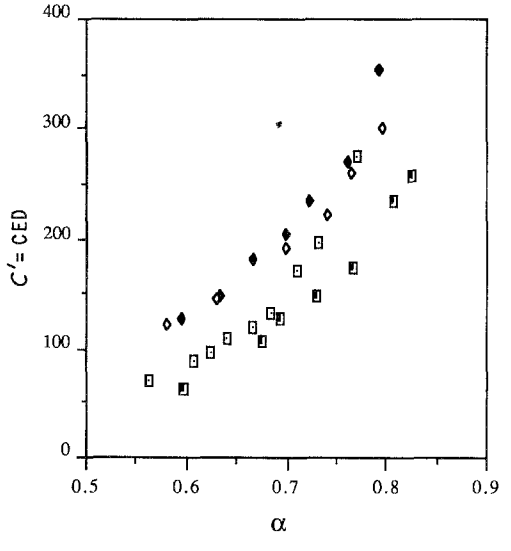

Figure 5 C' = CED plotted against α from experimental compliance determination of mini short-rod specimens. Specimen no.: (◇) 1, (◧) 2, (◆) 3, (□) 4.

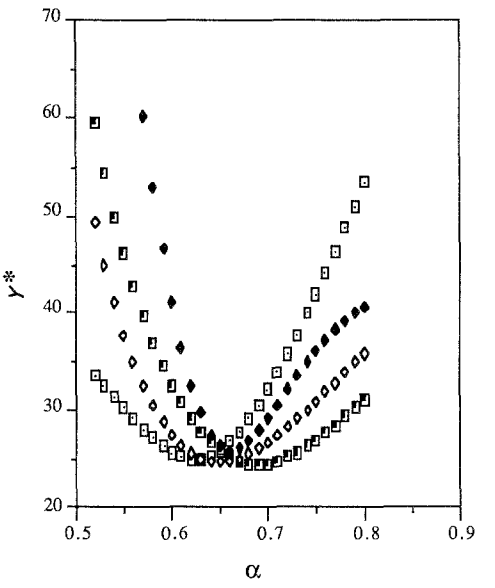

Figure 6 Stress intensity factor coefficient plotted against α experimentally determined for mini short-rod specimens. Specimen no.: (□) 1, (◆) 2, (◧) 3, (◇) 4.

a is shown in Fig. 6. Y_m^* and the corresponding a_m for this example can be determined from Fig. 6.

2.3.2. Plane-strain fracture toughness

Upon loading and unloading most specimens, slight hysteresis and nonlinear load–displacement behaviour occurred. To determine p, the load–unload curves were extrapolated to zero load using the initial linear portion of the loading curve as illustrated in Fig. 7. The choice of initial linear portion of the loading curve was considered appropriate because (1) only loading curves were used in our experiments to determine Y_m^*, so a better match between the extrapolated slope using the loading portion of the curve and Y^* should result, (2) near steady state stress–strain would have developed following stress-relaxation after the holding period following unloading; the p factors calculated from these linear extrapolations should, therefore, reflect only true plastic deformations, and (3) the extrapolated line defining the initial compliance of the specimen was drawn from the first loading curve after the conditioning cycle. Thus a consistent condition can be established if all extrapolations were performed using loading data only.

The method for calculating p is shown in Fig. 7. The

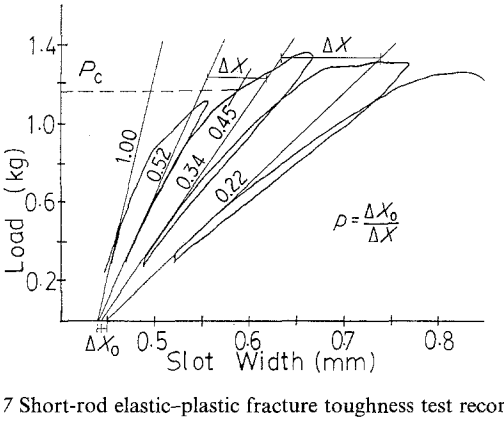

Figure 7 Short-rod elastic–plastic fracture toughness test record of a mini acrylic specimen.

TABLE I Experimentally determined minimum stress intensity factor coefficients and corresponding dimensionless critical crack length

Specimen no.	Y_m^*	a_m (mm)
1	24.6	0.670
2	23.9	0.705
3	25.3	0.705
4	23.7	0.650

plasticity factor is defined as $\Delta X_0/\Delta X$, where ΔX_0 is the displacement at zero load, and ΔX is the displacement between the two extrapolated lines at the average peak load of the two load–unload cycles. Because three load–unload cycles were performed, two p values were determined for each test and the average value was used for the calculation of K_{IC}.

The compliance calibration curves indicated that at a_m, the crack length corresponding to Y_m^*, the compliance of the mini short-rod specimen was 2.2 times the initial compliance. To determine the critical load, P_c, corresponding to a_m, second degree polynomials relating the slope of the extrapolated lines and slot opening were determined. Interpolating using the second degree polynomial by choosing a slope equal to 1/2.2 (=0.45) times the initial slope gave P_c.

3. Results

3.1. Stress intensity factor coefficient of the mini short-rod specimen

The value of Young's modulus for the acrylic used was determined to be 3.00 ± 0.15 GPa.

Values of Y^* were calculated using Equation 3 for a values increasing in 0.005 intervals between 0.450 and 0.800. Y_m^* and a_m values determined from Y^* against α curves are shown in Table I. Based on these results, with correction for craze zone length effect as discussed below, $Y_m^* = 25.0 \pm 0.06$ was used for the analysis of our mini test specimens.

3.2. Plane-strain fracture toughness of the extruded acrylic

The results of our fracture toughness testing acrylic are presented in Table II. Our experimental results can be compared to reported K_{IC} values for commercial PMMA determined using various plane-strain fracture toughness tests listed in Table II. It appears that K_{IC} values determined using the mini short-rod test are lower than the values reported by others. K_{IC} for our acrylic specimens measured using the short-rod EP fracture toughness test is 0.67 MPa m$^{1/2}$ with 10% standard deviation. A standard deviation of 10% is similar to that reported for PMMA testing using various methods, and is considered very good for fracture toughness testing of plastics where 40% deviation is common [22].

4. Discussion

4.1. Stress intensity factor coefficient minimum

Y_m^* can be calculated by rearranging equation 1

$$Y_m^* = \frac{K_{IC} DW^{1/2}}{P_c} \quad (4)$$

Barker determined Y_m^* for short-rod test specimens

TABLE II Comparison of K_{IC} values of commercial PMMAs obtained using mini short-rod and other test methods

Reference	Material	K_{IC} (MPa m$^{1/2}$)	Experimental details
Hill *et al.* [16]	Perspex sheet	1.3(0.03)	3 mm thick DT specimens
		1.15(0.03)	6 mm thick DT specimens
		1.12(0.11)	3 mm thick CT specimens
		0.99(0.05)	6 mm thick CT specimens
Stafford *et al.* [17]	Perspex	1.13(0.1)	TC specimens
		1.60(0.07)	SEN specimens
Barker [1]	Cast PMMA sheet	1.05	SR specimens, LE analysis
Burchil *et al.* [18]	Polycast 71	1.00	DT 30 mm × 80 mm specimens
	Plexiglas 55	1.07	as above
	Plexiglas 249	1.08	as above
	S-708	0.83	as above
	Plexiglas 201	0.99	as above
Watson *et al.* [19]	1 in. thick PMMA sheet	1.05(0.04)	CT specimens, 25 mm thick
		1.05(0.05)	SR specimen, with p correction
		0.82(0.05)	SR specimens, without p correction
Koblitz *et al.* [20]	Cast PMMA rod	1.00	6.39 mm diameter SR specimens, LE analysis
		1.00	12.75 mm diameter SR specimens, LE analysis
Hashemi and Williams [21]	High MW PMMA cast sheet	1.80	SEN specimen at 20° C three point bend
Freitag and Cannon [41]	Plexiglas II Sheet	1.26	SEN specimen
Present work	1/2 in. extruded PMMA rod	0.67(0.05)	Mini SR specimens with plasticity correction
		0.70(0.04)	Mini SR specimens without plasticity correction

DT = double torsion; CT = compact tension; TC = tapered cleavage; SEN = single-edge notched; SR = short-rod.

TABLE III Comparison of minimum stress intensity factor coefficients for various short-rod specimen geometries

Reference	Short-rod specimen geometry				Method*
	W/D	a_0 (mm)	a_1 (mm)	Y_m^*	
Barker [1]	1.45	0.31	0.96	26.3	a
Barker [24]	1.474	0.343	0.992	29.6	b
Barker [25]	1.45	0.31	0.96	25.1	a
Barker and Baratta [23]	1.45	0.343	0.992	26.5	a
Beech and Ingraffea [12]	1.50	0.35	1.00	31.2	c
Bubsey *et al.* [10]	1.45	0.332	1.00	29.0	b
Barker [3]	1.45	0.332	1.00	28.2	b
Shannon *et al.* [11]	1.45	0.332	1.00	29.1	b
Raju and Newman [8]	1.45	0.332	1.00	28.4	c
Ingraffea *et al.* [9]	1.45	0.332	1.00	28.3	d
Bubsey *et al.* [10]	1.653	0.421	0.950	33.1	b
Shannon *et al.* [11]	1.653	0.421	0.950	32.7	b
Barker [3]	1.653	0.421	0.950	32.1	b
Present work	1.653	0.421	0.950	25.0†	b

*Method: a, matching K_{IC} from ASTM-E399 derived values and short-rod test results; b, experimental compliance calibration; c, finite-element analysis; d, boundary-element analysis.
†Value corrected for craze zone length effect.

from Equation 4 by using a standard reference material, 2014-T651 aluminium, for which K_{IC} was known from standard ASTM-E399 testing and by measuring the peak load (P_c) in his short-rod fracture toughness test. The value of Y_m^* obtained using this procedure was 26.3 [1]. This value was increased 4% to 26.5 after further experiments on several steel, aluminium and titanium alloys [23].

Experimental compliance calibration curves were later determined by Bubsey *et al.* [10], Shannon *et al.* [11] and Barker [3] to ascertain Y_m^* for a family of short-rod specimens with different dimensions. Variation in the value of Y_m^* with specimen dimensions was expressed in the form of mathematical relationships. The minimum stress intensity factor coefficient for individual specimens that vary in geometry due to machining or moulding variations thus can be computed using these relationships.

A "standard" short-rod specimen geometry being investigated by the ASTM-E24 Committee for Fracture Toughness Testing has been analysed using finite element methods by Raju and Newman [8] and Ingraffea *et al.* [9]. The analysis modelled distributed loads acting on the front face of the specimen and assumed negligible slot widths. The experimental and the analytical results generally agreed to within 3% (Table III).

The minimum stress intensity factor coefficient for our mini short-rod specimen is approximately 17% lower than that determined for the "standard" specimen. Y_m^* is a function of specimen geometry and, therefore, comparisons between Y_m^* can only be made for fixed values of dimensionless specimen geometrical parameters such as W/D and a_0. Values of Y_m^* determined for different specimen geometries and by different methods (experimental and analytical) are listed in Table III.

Included in Table III are the experimentally determined values of Y_m^* for our miniature short-rod specimens. The Y_m^* values for the larger specimens near the bottom of the table [3, 10, 11] were extrapolated to correspond to specimens with a_0, a_1, and W/D equal to our miniature short-rod specimens. Our value of Y_m^* is lower than the values determined for the larger specimens (i.e. 25.0 compared to 32.7).

A number of factors could explain the difference in Y_m^* determined for our smaller specimens. First of all, the loading fixture employed for testing the mini short-rod specimens is different from that used by other investigators in testing larger short-rod specimens. With the larger specimens, loading can be achieved conveniently using a knife-edge loading fixture which distributes the load uniformly along the specimen cross-section. Our mini specimens were loaded through holes in the loading collar (Fig. 1) and this corresponds to a concentrated load acting at the centre line of the specimen. Finite element calibration of the short-rod specimen by Beech and Ingraffea [12] showed that Y_m^* is about 11.4% higher in the case of a uniformally distributed load acting on the specimen compared with point loading. This would partly explain the lower values of Y_m^* for our mini short-rod specimens.

A major concern in using acrylic (PMMA) as a material for determining Y_m^* as a calibration medium is the difficulty of measuring effective crack length because of crazing ahead of the crack tip. The craze zone in PMMA consists of cavities just ahead of the crack tip with interspersed ligaments of highly drawn fibrils of polymer. These fibrils join the two crack surfaces and are capable of supporting load. Because crazed material differs in refractive index from the bulk polymer, viewing the crack-tip through an optical microscope using normal incident light shows the craze zone as a set of interference fringes [13, 23, 26–28]. The crack length measurements that we used were taken at the last bright interference fringe, and, therefore, the craze zone is included in our measurements. It has been reported that the length of the craze region varies with stress intensity, and below a critical stress intensity of 0.3 to 0.4 MPa $m^{1/2}$ no craze zone is observed [13, 29]. For stress intensities between 0.4 and 1.0 MPa $m^{1/2}$ the craze zone length conforms to that predicted using a plane strain zone model [13]. The length of the craze zone in this stress intensity range can be predicted using the equation [13]

$$l_c = \frac{K_{IC}^2}{3\pi\sigma_{ys}^2} \quad (5)$$

where l_c is the craze zone length, K_{IC} is the stress intensity and σ_{ys} is the yield strength of the material. The craze zone length reaches a limiting value of 40 mm at higher stress intensity levels [13, 30]. In order to estimate an error in the determination of Y_m^* because of the uncertainty in effective crack length measurement (i.e. to what extent does the craze zone act as a crack extension?), craze lengths at different stress intensity levels were calculated using Equation 4 and subtracted from the measured crack length to obtain a new set of crack lengths against compliance data. Y_m^* calculated from this new data set is presented in Table IV. Comparing the two sets of Y_m^* values in Table IV indicates that they are significantly different ($p < 0.01$). Exclusion of craze lengths increases Y_m^*

TABLE IV Comparison of experimentally determined mini short-rod Y_m^* values corrected and uncorrected for craze zone effect

Specimen no.	Y_m^* (uncorrected for crazing)	a_m (mm)	Y_m^* (corrected for crazing)	a_m (mm)
1	24.6	0.670	24.6	0.650
2	23.9	0.630	24.5	0.560
3	25.3	0.705	25.9	0.660
4	23.7	0.650	25.0	0.625

by 6%. The effect might be greater yet, because the theoretical correction used (Equation 4) does not account for possible static craze growth. Williams and Marshall [27] have shown craze growth in PMMA tested in air at $K_I = 0.7\,MPa\,m^{1/2}$. Craze growth therefore could have occurred during testing, and its effect on the value of Y_m^* could be much larger than that predicted using Equation 4.

A possible source of error in Y_m^* determination relates to uncertainties of the crack front profile. Finite element analysis of short-rod specimens using a linear-elastic model has predicted higher stress intensities at the outer edges of the crack front [8, 9]. Based on this result, retardation of crack growth at the centre of the crack front is expected. As the crack progresses, however, a crack front profile with retardation of growth in the outer edges or "thumbnailing" is observed for the mini short-rod acrylic specimens. This profile can be rationalized through the relaxation of constraints at the free edge of the crack front leading to plane-stress conditions in these regions which has the effect of retarding crack growth. The net effect of the two opposing forces – higher stress intensity and increasing plasticity – at the outer edges of the crack front as it propagates depend on their relative magnitudes. In the mini acrylic specimens with short crack lengths the two forces apparently balance one another and a straight crack front was seen.

However, when longer crack lengths develop, the plastic zone at the free edges corresponding to the condition of plane-stress will increase in size as the crack grows and cause the retardation of the crack front at the outer edges. Material properties obviously have a strong influence on the rate of relaxation of constraint and, therefore, the curvature of the crack front that develops. The effect of using the average crack length of a curved crack front on the value of Y_m^* is not clear at present.

An argument can be made for using a material for experimental determination of Y_m^* that is similar to the material being tested using the short-rod EP fracture toughness test. This is especially true for polymeric materials which exhibit time-dependent properties, crazing, and higher levels of plasticity. For fracture toughness testing of PMMA or similar materials (i.e. bone cement, dental composites) using the mini short-rod EP method, it is proposed that the value of $Y_m^* = 25.0$ should be used in the determination of K_{IC}. For comparative studies in which the effect of processing variables or ageing is being assessed, and relative K_{IC} values are being determined, the absolute value of Y_m^* is not important. This is the case for our subsequent study on bone cement [6].

4.2. Plane-strain fracture toughness of extruded acrylic

A higher measured toughness value is expected if plane-strain conditions are relaxed during the fracture toughness test due to small transverse test specimen dimensions. However, the K_{IC} that we have determined for our acrylic specimens is lower than that reported by others for PMMA using larger specimens. A number of factors could explain the lower K_{IC} values determined in our studies compared to those reported by others.

The first possibility is related to crack-tip sharpness effect. Some researchers listed in Table II have measured fracture toughness of PMMA using specimens not properly fatigue precracked thus resulting in a blunted crack front which would be expected to give unrealistically high K_{IC} values.

Real differences in material processing and preparation are also suspect in the discrepancy of measured K_{IC} values. The mini short-rod specimens tested were machined from 12.5 mm diameter extruded commercial acrylic rod (Polymer, USA), whereas most other investigators prepared their specimens from cast sheets or rods obtained from various manufacturers. The process of forming an extruded rod tends to orient and stretch the molecular chains in the direction of extrusion resulting in an orthotropic material. A study of hot-stretched PMMA sheets [31] has shown that both static and cyclic crack growth resistance is improved if the crack propagates normal to the direction of stretching. Crack resistance in the direction parallel to hot stretching, however, is decreased. In the case of our mini short-rod specimens, the chevron notch was machined in the direction of the long axis of the rod, and, therefore, the crack propagated in the direction of extrusion. Based on the study of stretched PMMA sheets of Kitagawa *et al.* [31], this direction should correspond to a direction of lowered resistance to crack propagation. Differences might also be due to variations in minor additives between different commercial materials and molecular weight differences related to processing parameters. Several studies have shown that increases in molecular weight cause improvements in the fracture toughness of PMMA-based polymers [32, 33]. This is evident in comparing the K_{IC} value for high molecular weight PMMA obtained by Hashemi and Williams [21] with the other values presented in Table II. For the extrusion of acrylic, plasticizers are usually added. These could have a strong effect on K_{IC}. We had assumed that our acrylic was pure PMMA and, hence, results could be compared with values of K_{IC} determined for PMMA as reported in the literature. Obviously, further studies using well characterized materials are needed.

Experimental conditions also can influence the results of mechanical tests. For a viscoelastic material such as PMMA, loading rate is especially important due to the time dependence of its mechanical properties. The cross-head speed employed for our short-rod fracture toughness test is similar to that chosen by other researchers listed in Table II. However, viscoelastic behaviour of the test material is dictated by strain rate, and our mini specimens being much shorter

than the others was effectively strained at a higher rate during the test. Sutton, experimenting with acrylic plastic, has shown a rapid decrease in K_{IC} of the test material with increased strain rate [34]. Lower K_{IC} results from our tests, therefore, can be explained by the higher strain rates employed.

The average plasticity correction factor, $\{(1 + p)/(1 - p)\}^{1/2}$, is 0.95 ± 0.07. The value of this factor being essentially unity indicates that the plastic zone at the crack tip during testing is small, thus satisfying the criterion of linear-elastic material behaviour for Y_m^* determination. This finding contradicts that observed by Watson *et al.* [19] who showed an average plasticity correction value of 1.32 for PMMA tested using larger short-rod specimens. Small plasticity, however, was to be expected from our specimens as the annealing process drives out any trapped water molecules (a plasticizer) within the polymer thereby lowering the material's plasticity [27]. Reduced plasticity decreases energy dissipation during fracture which could also have contributed to lower our measured K_{IC} value as compared with the others. High plasticity observed by Watson *et al.* [19] may also be due to the lack of a relaxation period in their loading and unloading of the specimens. Viscoelastic behaviour of PMMA, therefore, was included in their calculation. Longitudinal compressive residual stress in the specimen not relieved by annealing may account for the fact that our plasticity correction is less than 1 [35]. No other test method accounts for the effect of residual stress. Thus, Watson *et al.* [19] and Wang *et al.* [36] suggested that an uncorrected value of K_{IC} should be used when comparing the results of the short-rod EP test and that determined using other methods. If this assertion is correct, our uncorrected K_{IC} value for PMMA would be $0.70\,\text{MPa}\,\text{m}^{1/2}$.

One of the basic assumptions in the development of the short-rod fracture toughness test is that the test material has a flat R-curve [1, 2]. Most brittle materials that this test was originally intended for satisfy this assumption. By extending the range of test materials to include materials with non-flat R-curves, such as PMMA, problems arise. Fig. 8 shows the relationship between Y^*, P and K_I for an ideal material with a flat R-curve. The maximum load applied to the specimen (P_c) corresponds to the minimum in Y^* (Y_m^*). Thus, K_{IC} can be calculated using the linear-elastic relationship of Equation 1. A material with a rising R-curve, however, shifts the maximum load in relation to the Y^* curve as indicated in Fig. 9 [37]. Therefore, if K_{IC} is calculated assuming a flat R-curve (Equation 1), the computed K_{IC} will lie on the K_I curve between K_{IC} and K_{max}. This situation can be remedied using the elastic–plastic analysis. The critical load, P_c, used in the EP analysis (Equation 2) is determined from the slopes of the load–unload cycles on the load–displacement curve and it corresponds uniquely to a_m and, therefore, Y_m^*.

One other difficulty associated with short-rod testing of non-flat R-curve materials exists. It is evident from Fig. 9 that the value of K_{IC} calculated for a rising R-curve material will depend on the amount of crack extension to a_m. The larger the specimen, the further

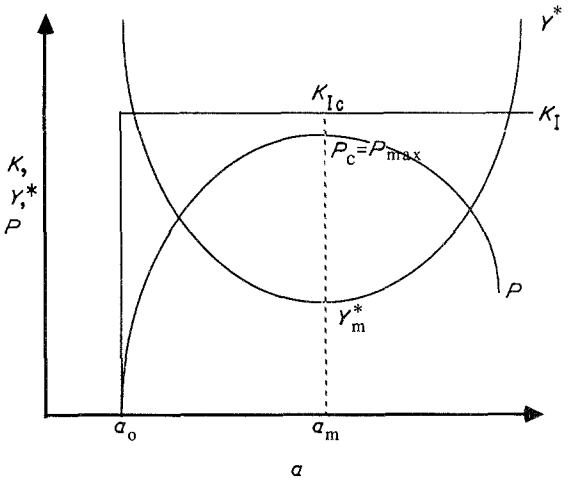

Figure 8 Schematic drawing showing the relationship between K, Y^*, and P plotted against a for an ideal elastic flat R-curve material.

the crack will have to propagate before reaching Y_m^* and, therefore, the higher will be the resulting K_{IC} value. Conversely, for a falling R-curve material, larger specimens will result in lower K_{IC} values when using the short-rod test. The R-curve for PMMA increases with crack velocity due to increased secondary crack formation at higher velocities [38, 39]. It is, therefore, difficult to predict the trend in K_{IC} with respect to specimen size without a knowledge of the crack velocity as the crack propagates through the specimen, especially at the point of K_{IC} measurement. ASTM-E399 standard tests measure the crack initiation toughness and, therefore, K_{IC} values so obtained are not strongly affected by the slope of the R-curve. There is no reason why we cannot mimic the ASTM standard tests using the short-rod EP test by choosing a Y^* corresponding to a short crack length sufficiently close to a_0 for the purpose of K_{IC} calculation using Equation 2. The mini short-rod specimen, due to its small size and therefore short crack propagation length, should be well suited for this purpose. In this case P_c would not be the load when the extrapolated compliance slope is 1/2.2 (= 45%) of the initial slope, but would correspond to some arbitrary early part of the test (95% of the initial slope for example).

Load–displacement curves from experiments on

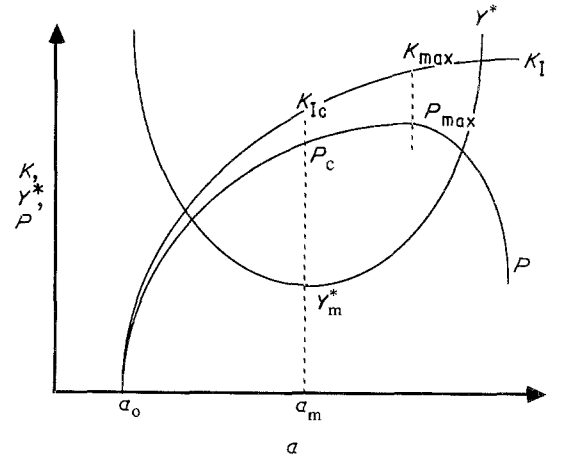

Figure 9 Schematic drawing showing the relationship between K, Y^* and P plotted against a (the lack of coincidence between P_{max}, Y_m^* and a_m) for a rising R-curve material after [37].

acrylic indicated this material behaved almost linear elastically as one would expect considering its brittleness. Some deviation from linear elasticity, however, can be observed which correspond to reported non-linear behaviour of PMMA [40]. The critical load, P_c, determined from experiments on the extruded acrylic were generally very close to the peak load applied to the specimens, being 2 or 3% below that value (see Fig. 7). Using the LE analysis method of the short-rod test, i.e. using Equation 1, would, therefore, have resulted in a K_{IC} value 2 to 3% higher than that reported here. This study has demonstrated that the elastic–plastic analysis can be used for determination of K_{IC} using the miniature short-rod fracture toughness specimens.

5. Conclusions

1. A method has been described to determine the plane-strain fracture toughness of materials with elastic–plastic correction using miniature short-rod specimens. For the acrylic specimens tested, this results in a slightly lower value of K_{IC} than would have been determined assuming linear-elastic behaviour. The result of our short-rod EP fracture toughness test using miniature test specimens indicates that K_{IC} of the extruded PMMA is $0.67 \pm 0.06\,\text{MPa}\,\text{m}^{1/2}$.

2. The minimum stress intensity factor coefficient for our mini short-rod specimen has been experimentally determined using extruded acrylic specimens to be $Y_m^* = 25.0 \pm 0.6$.

3. Non-flat R-curve materials (such as PMMA) present a problem for short-rod fracture toughness testing as the K_{IC} value obtained from such a test is crack length, hence, specimen size dependent. A modification to the test procedure, using a Y^* value corresponding to a short crack length sufficiently close to a_0, is suggested as a method of overcoming this difficulty.

References

1. L. M. BARKER, *Eng. Fract. Mech.* **9** (1977) 361.
2. *Idem*, *Int. J. Fract.* **15** (1979) 515.
3. *Idem*, *Eng. Fract. Mech.* **17** (1983) 289.
4. R. M. PILLIAR, D. F. WILLIAMS and R. VOWLES, in "MRS Symposium Proceedings Vol. 55, Biomedical Materials" edited by J. M. Williams, M. F. Nichols and W. Zingg (MRS, Pennsylvania, 1986) p. 369.
5. L. M. BARKER, in ASTM STP 855 (American Society of Testing and Materials, Philadelphia, Pennsylvania, 1984) p. 117.
6. C. T. WANG and R. M. PILLIAR, *J. Mater. Sci.*
7. D. MUNZ, R. T. BUBSEY and J. E. SRAWLEY, *Int. J. Fract.* **16** (1980) 359.
8. I. S. RAJU and J. C. NEWMAN Jr, in ASTM STP 855 (American Society of Testing and Materials, Philadelphia, Pennsylvania, 1984) p. 32.
9. A. R. INGRAFFEA, R. PERUCCHIO, T. Y. HAN, W. H. BERSTLE and Y. P. HUANG, in ASTM STP 855 (American Society of Testing and Materials, Philadelphia, Pennsylvania, 1984) p. 49.
10. R. T. BUBSEY, D. MUNZ, W. S. PIERCE and J. L. SHANNON Jr, *Int. J. Fract.* **18** (1982) 125.
11. J. L. SHANNON Jr, R. T. BUBSEY, W. S. PIERCE and D. MUNZ, *ibid.* **19** (1982) R55.
12. J. F. BEECH and A. R. INGRAFFEA, *ibid.* **18** (1982) 217.
13. S. J. ISREAL, E. L. THOMAS and W. W. GERBERICH, *J. Mater. Sci.* **14** (1979) 2128.
14. R. M. PILLIAR, R. VOWLES and D. F. WILLIAMS, *J. Biomed. Mater. Res.* **21** (1987) 145.
15. R. M. PILLIAR, D. C. SMITH and B. MARIC, *J. Dental Res.* **65** (1986) 1308.
16. R. G. HILL, J. F. BATES, T. T. LEWIS and N. REES, *Biomater.* **4** (1983) 112.
17. D. STAFFORD, R. HUGGET and B. E. CAUSTON, *J. Biomed. Mater. Res.* **14** (1980) 359.
18. P. J. BURCHILL, G. MATHYS and R. H. STACEWICZ, *J. Mater. Sci.* **22** (1987) 483.
19. T. WATSON, M. JOLLES, P. PEYSER and S. MOSTOVOY, *ibid.* **22** (1987) 1249.
20. F. F. KOBLITZ, V. R. LUNA, J. F. GLENN, K. L. DeVRIES and R. A. DRAUGHN, *Polym. Engng Sci.* **19** (1979) 607.
21. S. HASHEMI and J. G. WILLIAMS, *J. Mater. Sci.* **19** (1984) 3746.
22. J. P. BERRY, in "Fracture", edited by H. Liebowitz (Academic, New York, 1972) p. 38.
23. L. M. BARKER and F. I. BARATTA, *J. Test. Eval.* **8** (1980) 97.
24. L. M. BARKER, *Int. J. Fract.* **17** (1981) R3.
25. *Idem*, *ibid.* **15** (1979) 515.
26. R. P. KAMBOUR, *J. Polym. Sci.* **A24** (1976) 349.
27. J. G. WILLIAMS and G. P. MARSHALL, *Proc. R. Soc. Lond.* **A342** (1975) 55.
28. G. P. MORGAN and I. M. WARD, *Polymer* **18** (1977) 87.
29. G. P. MARSHALL, L. E. CULVER and J. G. WILLIAMS, *Proc. Roy. Soc. Lond.* **A319** (1970) 165.
30. H. R. BROWN and I. M. WARD, *Polymer* **14** (1973) 469.
31. M. KITAGAWA, H. DAJIWARA, H. KANZAKI and T. ZHANG, *J. Mater. Sci.* **20** (1985) 1945.
32. R. P. KUSY and D. T. TURNER, *Polymer* **18** (1977) 391.
33. S. A. BROWN and W. L. BARGAR, *J. Biomed. Mater. Res.* **18** (1984) 523.
34. S. A. SUTTON, *J. Test. Eval.* **6** (1978) 356.
35. L. M. BARKER, in "Advances in Fracture Research", Vol. 5, edited by D. Francois (Pergamon, Exeter, 1981) p. 2563.
36. C. WANG, M. YUAN and T. CHEN, in ASTM STP 855 (American Society of Testing and Materials, Philadelphia, Pennsylvania, 1984) p. 193.
37. J. L. SHANNON Jr and D. G. MUNZ, in ASTM STP 855 (American Society of Testing and Materials, Philadelphia, Pennsylvania, 1984) p. 270.
38. N. OHTANI and A. KOBAYASHI, *J. Appl. Polym. Sci.* **29** (1984) 1537.
39. A. KOBAYASHI and N. OHTANI, *ibid.* **24** (1979) 2255.
40. B. POURDEYHIMI, H. D. WAGNER and P. SCHWARTZ, *J. Mater. Sci.* **21** (1986) 4468.
41. F. A. FREITAG and S. L. CANNON, *J. Biomed. Mater. Res.* **10** (1976) 805.

Received 22 August
and accepted 27 September 1988